Chapter 7

Low-Noise Amplifiers

The history of high-frequency receivers is largely the history of the search for low noise. One of the most important goals—and successes—of the MIT Radiation Laboratory, during the 1940s, was the improvement of the sensitivity of radar receivers. Throughout the 1960s and 1970s, as space communication matured, the search for low-noise diode mixers became critical. The development of low-noise microwave FET devices, and their improvement to the point of astonishingly low noise figures, was one of the major technological successes of the 1980s and 1990s.

Even though we now have extraordinarily good low-noise transistors, the problem of optimization is just as important as in the past. Indeed, there is no point in incurring the huge expense and effort of developing such devices if designers do not create circuits that realize those devices' potential. This chapter addresses that subject.

In this chapter, we are concerned exclusively with high-frequency noise. Low-frequency noise, both $1/f$ and burst noise, although present in the devices we discuss, is invariably too low in frequency to affect high-frequency amplifiers. These noise sources become important in nonlinear circuits, especially oscillators, which we examine in other chapters.

7.1 FUNDAMENTAL CONSIDERATIONS

7.1.1 Solid-State Devices

Both bipolar and FET devices are used in high-frequency amplifiers. Homojunction bipolar devices and silicon FET devices are generally suitable for use at frequencies up to a few gigahertz; some advanced technologies, especially short-gate silicon MOS devices, may be useful well into the mi-

crowave or even millimeter regions. The minimum noise figures of devices realized in III-V technologies are significantly lower than those in silicon, however. This is especially true of high-electron-mobility transistors (HEMTs) and pseudomorphic HEMTs, sometimes called pHEMTs. These offer extraordinarily low noise figures. The most advanced pHEMT technologies can operate into the high end of the millimeter-wave region. Heterojunction bipolar devices (HBTs) are also used at microwave frequencies. Their noise figures are inferior to FETs, however, so they are used primarily for low-distortion and large-signal operation.

At this writing, HEMT devices have almost completely supplanted conventional GaAs MESFETs for low-noise microwave applications. The higher electron mobility in HEMTs, combined with process optimization to reduce resistive parasitics, is largely responsible for their low noise figures. This advantage comes at a cost: HEMT devices operate at very low currents, giving them, at best, limited ability to handle large signals. They also exhibit a stronger transconductance nonlinearity, giving them higher levels of distortion than conventional MESFETs.

7.1.2 DC Bias

In both FET and bipolar devices, the minimum noise figure and other noise parameters (Section 5.2) are functions of the drain or collector current, as appropriate. As we shall see in Section 7.1.3, the noise figure is, among other effects, a function of (1) the input mismatch and (2) an interplay between the gain and output noise current. We examine these effects as they apply to FET and bipolar devices.

7.1.2.1 Bipolar Devices

In all bipolar devices, the dominant high-frequency noise source, beyond the obvious thermal noise of parasitic resistances, is shot noise in the collector current. The mean-square value of shot-noise current, from (2.53), is proportional to dc collector bias current, I_{cc}. The transconductance, g_m, at low to moderate collector currents, is proportional to I_{cc} as well, but the gain is proportional to g_m^2. Thus, at small collector currents, noise figure decreases as I_{cc} increases.

As I_{cc} increases further, the gain peaks and eventually decreases, so noise figure increases. This peak has a number of causes. In all devices, the gain cannot increase significantly beyond the point where g_m exceeds the inverse of the emitter parasitic resistance. Thermal effects and high-level injection effects (in silicon devices) also decrease the gain at high current.

As an example, Figure 7.1 shows the measured gain ($|S_{21}|^2$) and minimum noise figure of a small-signal silicon BJT at 2 GHz as a function of collector current. The gain peak occurs at 10 mA, but leveling is evident at somewhat lower current levels. The noise figure exhibits a broad minimum in the 2- to 6-mA range.

Bipolar devices, especially in silicon homojunction technologies, have relatively high base resistances compared to the gate resistances of microwave FETs. This makes the base resistance a significant noise source. The greater input resistances, along with their lower current gain-bandwidth products, ω_t (Section 7.1.3.2), are responsible for their higher noise figures.

7.1.2.2 FET Devices

As with bipolar devices, the noise figure of a FET is established by an interplay between gain, drain noise current, and thermal noise of the parasitic resistances, especially the gate and source resistances. In low-frequency MOSFETs and JFETs, the channel noise arises largely from thermal noise in the undepleted channel. In MESFETs, HEMTs, and short-channel silicon devices, however, high-field diffusion noise increases the channel noise beyond the thermal component.

The transconductance of most FETs is a much weaker function of bias current than in bipolars, but, especially in high-frequency devices, the nonthermal channel noise is a relatively strong function. As a result, the optimum noise figure of most FETs occurs at a low current, typically 15% to at

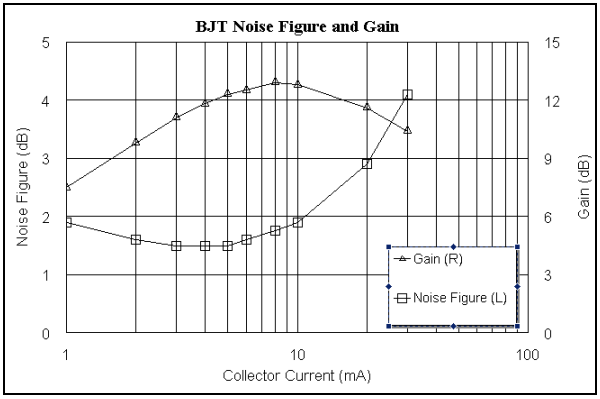

Figure 7.1 Measured noise figure and gain of a silicon bipolar transistor chip at 2 GHz.

most 25% of the maximum drain current. In microwave FETs, this is approximately 1 to 2 dB below the current that provides maximum gain and well below the level that provides the lowest distortion. Optimizing the noise figure of a FET amplifier frequently involves a painful trade-off between gain, distortion, and noise.

The gate and source parasitic resistances of microwave FETs are much lower than the base and emitter resistances of microwave BJTs. This, and the substantially higher current gain-bandwidth product, in spite of greater nonthermal drain noise, is the main reason for the superior performance of microwave FET devices.

7.1.3 Low-Noise Matching

7.1.3.1 Fundamental Considerations

In this section we address the problem of optimizing an amplifier's matching networks. We assume that the transistor can be treated as a linear two-port, and that its noise parameters and scattering parameters are available to the designer.

In Section 5.2 we made the point that the noise figure of a two-port depends on its noise parameters, $F_{\min}$, R_n, and $Y_{s,\,\mathrm{opt}}$, and the source admittance, Y_s. The most common form of the expression relating noise figure, F, to source admittance is

$$F = F_{\min} + \frac{R_n}{G_s}\left|Y_s - Y_{s,\,\mathrm{opt}}\right|^2 \tag{7.1}$$

where $F_{\min}$ is the minimum noise figure, R_n is the noise resistance, $Y_{s,\,\mathrm{opt}}$ is the source admittance that provides minimum noise figure, and $G_s = \mathrm{Re}\{Y_s\}$. The noise parameters vary with both dc bias and frequency. Beyond device selection, the noise parameters are largely out of the designer's control, so optimization of low-noise amplifiers largely involves optimizing the dc bias and source admittance. This task is straightforward in the case of narrowband amplifiers, but somewhat less obvious for broadband amplifiers.

Noise figure is independent of lossless output matching. Real matching networks invariably have loss. Input loss must, of course, be minimized; often it can be kept low enough to have a negligible effect on the amplifier's noise figure. The effect of output loss on noise figure is usually negligible, unless resistive loading or some other lossy technique (e.g., to enhance stability) is used in the output network. Then the noise introduced

by the loading may be significant, although still much less than the same loss located at the input. Many amplifiers can be stabilized by adding resistors in either the input or output matching circuits; clearly, in low-noise amplifiers, they should be used only in the output, if at all.

Feedback can affect the noise parameters of a two-port (Section 5.2). Feedback can sometimes improve the input VSWR when the amplifier is noise-matched; one common technique is the use of inductance in series with the source terminal. Source inductance increases the real part of the transistor's input impedance, while affecting the minimum noise figure only slightly. Source inductive feedback is used almost exclusively in FET amplifiers; it is generally not practical or necessary in bipolar amplifiers.

7.1.3.2 Optimum Source Admittance

Realizing a source impedance as close as possible to $Y_{s,\,\mathrm{opt}}$ is the most important aspect of low-noise amplifier design. Thus, we need to know $Y_{s,\,\mathrm{opt}}$. $Y_{s,\mathrm{opt}}$ can be measured or, with a noise model of the device, calculated. Synthesizing the optimum $Y_{s,\,\mathrm{opt}}$ over a prescribed bandwidth, with minimum circuit loss, is then an exercise in matching-circuit design.

Intuitively, one might expect $Y_{s,\mathrm{opt}}$ to be a conjugate match to the device's input impedance. It may be surprising to discover that, in general, it is not; in fact, minimizing noise figure usually requires a significant input mismatch. We can demonstrate the reason for this situation through an heuristic examination of a FET's noise equivalent circuit.

To demonstrate the effect of input matching, we examine the simple FET amplifier circuit of Figure 7.2. The circuit does not include some important parasitics, notably the source-terminal resistance and feedback capacitance; these would complicate the analysis and its interpretation, but would not change the fundamental results. Noise is modeled in a manner similar to that of Pospieszalski (Section 4.4.3). The circuit contains two noise sources: a thermal noise source at the input associated with the resistance R_i, v_{ni}, and a nonthermal noise source between the drain and source, representing channel noise, i_{nd}. We assume that the input reactance is matched, so $\omega L_s = 1 / C_{gs}\omega$; this is clearly optimum, a consequence of removing all of the usual feedback elements. If we had included a feedback capacitance and source-lead inductance and resistance, a different reactance might be needed. We also assume the output to be conjugate matched, so $R_L = R_{ds}$ and $\omega L_L = 1 / C_{ds}\omega$. This latter assumption is not strictly necessary, but it simplifies the analysis and interpretation of the results.

We begin by setting $i_{nd} = 0$ to examine the effect of input matching in the absence of channel noise. Since the circuit to the right of the input loop is noiseless, we need not include it in the calculations, and we need only

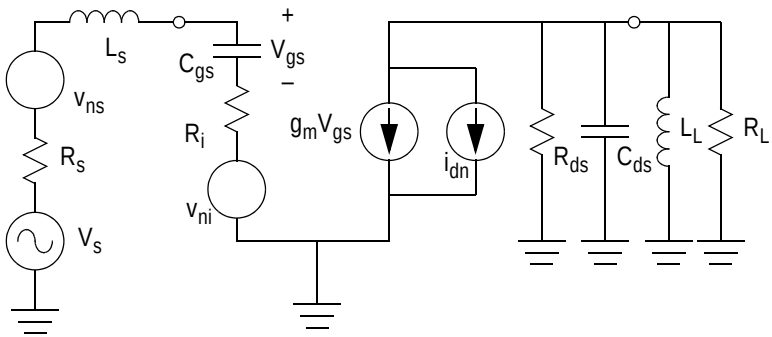

Figure 7.2 Simplified FET equivalent circuit used in the noise analysis of Section 7.1.3.2.

consider the voltage across C_{gs} as a function of the noise voltages. The noise figure [(3.9) and (5.22)] is

$$F = \frac{\overline{|i_{L,\,\mathrm{tot}}|^2}}{\overline{|i_{L,\,s}|^2}} = \frac{\overline{|v_{c,\,\mathrm{tot}}|^2}}{\overline{|v_{c,\,s}|^2}} \tag{7.2}$$

where $i_{L,\,\mathrm{tot}}$ is the total output current in the load and $i_{L,\,\mathrm{s}}$ is that portion of the current engendered by the source noise. $v_{c,\,\mathrm{tot}}$ and $v_{c,\,s}$ are analogous voltages at C_{gs}. Then

$$v_{c,\,\mathrm{tot}} = \frac{v_{ni} + v_{ns}}{(R_i + R_s)C_{gs}\,j\omega} \tag{7.3}$$

Since v_{ni} and v_{ns} are uncorrelated, they combine in a mean-square sense:

$$\overline{|v_{c,\,\mathrm{tot}}|^2} = \frac{\overline{|v_{ni}|^2} + \overline{|v_{ns}|^2}}{(R_i + R_s)^2 C_{gs}^2\,\omega^2} \tag{7.4}$$

Similarly,

$$\overline{|v_{c,\,s}|^2} = \frac{\overline{|v_{ns}|^2}}{(R_i + R_s)^2 C_{gs}^2 \omega^2} \tag{7.5}$$

and from (7.2),

$$F = 1 + \frac{\overline{|v_{ni}|^2}}{\overline{|v_{ns}|^2}} = 1 + \frac{R_i}{R_s} \tag{7.6}$$

This result tells us that, under the stated assumptions, we can achieve an arbitrarily low noise figure by increasing R_s. In fact, a conjugate match ($R_i = R_s$) produces an uninspiring 3-dB noise figure. This intuitively unsatisfying conclusion, that an input mismatch can produce an arbitrarily low noise figure, occurs only because we have assumed away the output noise. In any case, it is something of a Pyrrhic victory; the mismatch $R_s \gg R_i$ eventually reduces the amplifier's transducer gain to impractically low values. Furthermore, as the gain decreases, the signal level in the drain circuit likewise decreases, so the effect of any noise in the drain circuit becomes progressively greater. We shall examine this effect in detail shortly.

Still, this exercise shows that mismatching the input of an amplifier, to some degree, is necessary for optimizing the noise figure. It is not difficult to see why this is so. The input signal voltage, V_s, is

$$V_s = \sqrt{8 P_{\text{av}} R_s} \tag{7.7}$$

so by increasing the source impedance, with a constant available power P_{av}, we effectively increase the signal voltage relative to v_{ni}. This increases the signal-to-noise ratio, and that increase is reflected in a decrease in noise figure. In fact, many kinds of low-frequency FET amplifiers, where the maximum available gain is high and C_{gs} is small, achieve surprisingly low noise figures in this manner.

The need for a high source impedance is a consequence of the series structure of the input circuit. If our input model were a shunt conductance with a current source, a low source impedance would optimize the noise figure.

We can derive a more realistic expression for the noise figure by including the drain noise source, i_{nd}. We now have

$$\overline{|i_{L,\,\mathrm{tot}}|^2} = \frac{1}{4}\left(g_m^2 \frac{\overline{|v_{ni}|^2} + \overline{|v_{ns}|^2}}{(R_i + R_s)^2 C_{gs}^2 \omega^2} + \overline{|i_{nd}|^2} \right) \tag{7.8}$$

$$|i_{L,\,s}|^2 = \frac{1}{4}\left(g_m^2 \frac{\overline{|v_{ns}|^2}}{(R_i + R_s)^2 C_{gs}^2 \omega^2} \right) \tag{7.9}$$

We obtain, from (7.2),

$$F = 1 + \frac{R_i}{R_s} + \frac{(R_i + R_s)^2 C_{gs}^2 \omega^2 G_{nd}}{g_m^2 R_s} \tag{7.10}$$

where G_{nd} is the noise conductance associated with i_{nd} (5.18). It is illustrative to convert (7.10) into the form,

$$F = 1 + \frac{R_i}{R_s} + \left(\frac{\omega^2}{\omega_t^2}\right) \frac{(R_i + R_s)^2 G_{nd}}{R_s} \tag{7.11}$$

where

$$\omega_t = \frac{g_m}{C_{gs}} \tag{7.12}$$

ω_t is the current gain-bandwidth product of the device. This quantity, expressed as the temporal frequency $f_t = \omega_t / 2\pi$, is a commonly used figure of merit.

Even though it applies to a simplified equivalent circuit, (7.11) provides a valid, intuitive sense of how a FET's noise figure depends on source impedance and frequency. As R_s increases, the term R_i / R_s decreases and rapidly becomes negligible, but the more complex term increases asymptotically in proportion to R_s. At low frequencies, where $\omega \ll \omega_t$, it is possible to minimize the noise figure by the use of a large value of R_s, but at high frequencies, the significance of the latter term limits the allowable values.

The optimum value of R_s can be determined by differentiating (7.11). This exercise results in an expression that is probably too complex to be intuitively useful. Instead, we calculate the noise figure as a function of fre-

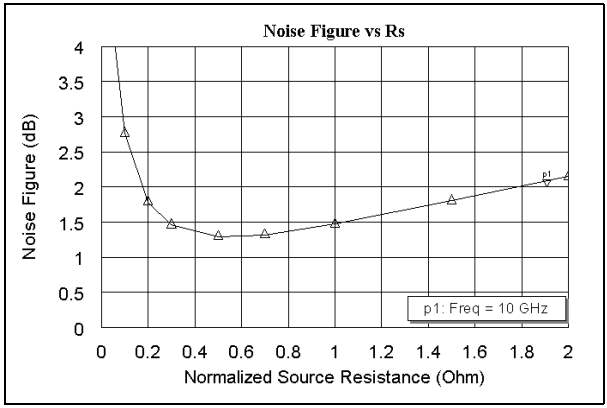

Figure 7.3 Noise figure of the circuit in Figure 7.2 at 10 GHz as a function of R_s, normalized to 50Ω. The circuit parameters are R_i = 4Ω, C_{gs} = 0.25 pF, g_m = 100 mS, and i_{nd} = 60 pA / Hz$^{0.5}$.

quency and R_s numerically; the result is shown in Figure 7.3. We also plot $Y_{s,\,\mathrm{opt}}$ as a function of frequency. The result, which looks much like many FETs' measured data, is shown in Figure 7.4(a).

$F_{\min}$ and R_n are shown in Figure 7.4(b). The plot of $F_{\min}$ may be different from what is normally found on transistor data sheets. Data sheets usually show a constant value of $F_{\min}$ at low frequencies. In fact, as the foregoing derivation showed, a microwave FET is virtually an ideal voltage-controlled current source at low frequencies, so its minimum noise figure theoretically approaches 0 dB. Unfortunately, $R_s \to \infty$ achieves this. Transistor data sheets instead show measured data, which is limited to practical values of R_s.

Figure 7.4(b) gives some insight as to the difficulty in optimizing the input match of a FET. The noise resistance, R_n, is relatively flat with frequency, approximately 27Ω. The theoretical minimum noise resistance, given by (5.29), varies smoothly from approximately 13 to 18 ohms from the low end of the frequency range to the upper end. This relatively high noise resistance makes FETs difficult to optimize over a broad bandwidth. Because of the inevitable difficulties in broadband matching, broadband FET amplifiers are usually matched best at the high end of the passband, where $F_{\min}$ is highest, and suffer greater noise-figure degradation at the low end, where $F_{\min}$ is lower and imperfection is more tolerable.

This analysis also provides some insight into the dependence of noise figure on bias. Up to a point, the FET's transconductance—and, thus, its ω_t—increases with drain current. This is especially pronounced in HEMT devices, which exhibit a distinct peak in transconductance with drain current. Unfortunately, G_{nd} also increases rapidly with drain bias current.

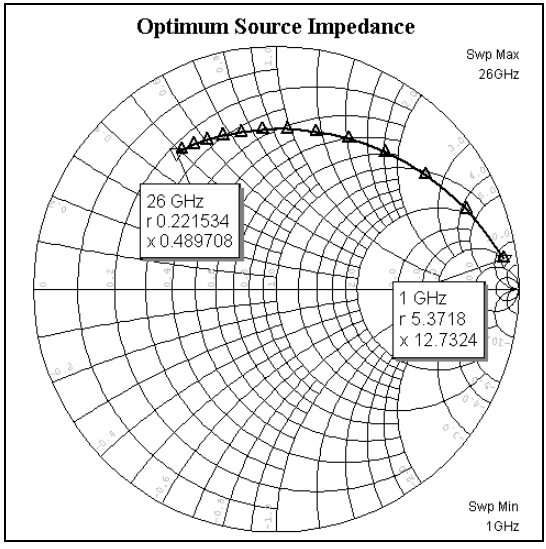

(a)

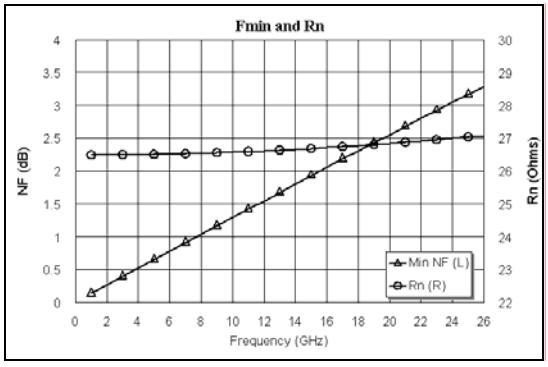

(b)

Figure 7.4 (a) Optimum source impedance as a function of frequency for the circuit in Figure 7.2, 1 to 26 GHz; (b) $F_{\min}$ and R_n. The circuit parameters are $R_i = 4\Omega$, $C_{gs} = 0.25$ pF, $g_m = 100$ mS, and $i_{nd} = 60$ pA / Hz$^{0.5}$.

These effects result in a relatively low optimum bias current, usually 15% to 25% of the peak drain current. This is well below the current required for low distortion, and results in gain 1 to 2 dB lower than is achievable at higher bias current.

7.1.3.3 Induced Gate Noise

Induced gate noise exists in high-frequency FETs, but its significance is still unclear. The Pucel model (Section 4.4.4) was developed with gate noise a clear consideration, but the Pospieszalski model (Section 4.4.3) does not include it. BSIM4, however, (Section 4.3.4) includes an induced-noise component.

The effect of gate noise is to include a component of noise in the gate that is correlated with the drain noise. If such noise is indeed significant, it complicates the above analysis, which now must account for the correlation. This modifies the value of the optimum source impedance somewhat, but, because the correlation is relatively small, the general conclusions of that analysis are still valid.

7.1.4 Input Losses

We noted in Chapter 3 that, in a cascade of two-ports, the first stage dominates in establishing the noise figure. When the first stage is lossy, its effect is especially deleterious. This point is evident immediately from Friis' formula for the noise figure of cascaded stages, (3.12). Although this formula was intended for matched stages, it is still valid for mismatched stages if the gain is defined as the available gain of each two-port [7.1]. The available gain, G_a, is

$$G_a = \frac{P_{\text{av},\,o}}{P_{\text{av},\,s}} \tag{7.13}$$

where $P_{\text{av},\,s}$ is the power available from the source and $P_{\text{av},\,o}$ is the power available from the output port of the two-port.

Losses can arise from power dissipation in imperfect components of the matching network or from radiation. Mismatch losses (such as an imperfect connector interface) do not introduce noise, but they can increase the noise figure by changing the source admittance presented to the device. Radiation losses are especially troublesome to deal with. Any circuit that radiates can also act as an antenna, receiving nonthermal noise and interference of various kinds. Placing the circuit in a metal housing may reduce

such spurious reception, but the metal cover and sidewalls can also change the characteristic impedances and phase velocities of microstrip conductors, thus changing the source impedance presented to the device. A housing can also increase input-to-output coupling, which can degrade stability and change the values of the device's noise parameters. Although a metal housing eliminates radiation from matching circuits, the design of the matching circuits should account for its effects.

7.1.4.1 Effect of Loss on Matching

In the design of a low-noise amplifier, we attempt to create a lossless input matching circuit. Then, the admittance of the source (i.e., the standard admittance Z_0) is transformed to some impedance $R_S + j\,X_S$ at its output terminals. The available power from that transformed source impedance is the same as that from the standard source.

Real matching circuits, of course, always have some loss. If the loss is small, the transformed impedance is not changed significantly, and the only effect is the increase in noise figure given by Friis' formula, with appropriate consideration for the points made in Section 3.1.5. If losses are greater, however, the source impedance $R_S + j\,X_S$ is also somewhat perturbed from the lossless value. In that case, generalizations are difficult, and a complete analysis of the input circuit is necessary to predict the amplifier's noise figure.

7.1.4.2 Lumped-Element Circuits

In many types of amplifiers, lumped-element matching, or integration of lumped elements with distributed circuits, may be practical. Lumped-element circuits are helpful in minimizing size, especially in integrated circuits and at low frequencies.

Although they are theoretically reactive elements, all types of lumped capacitors and inductors have inherent losses. The losses in wirewound inductors come primarily from the resistance of the wire, increased at high frequencies by skin effect. Large inductors can radiate, so they usually must be enclosed in some way. Losses in chip capacitors result from both the resistivity of their plates and loss in their dielectrics. Although dielectric loss usually dominates, both can be significant, depending upon frequency and the structure of the component.

In any matching circuit, certain components carry higher currents than others. The high-current components are usually at the low-impedance end of the matching circuit. These components should have the highest Q possible. Using a pair of parallel-connected chip components in high-current

parts of the circuit, instead of a single component, often reduces losses, because the series resistance of chip components often is relatively constant with their values. This is especially true of capacitors (less so of wirewound inductors), so using two half-value capacitors in parallel decreases their combined series resistance to approximately half that of a single capacitor.

Planar lumped elements realized in integrated-circuit processes are notoriously lossy. In planar spiral inductors, metal losses are relatively high because defects, such as edge roughness in the conductors, are relatively large compared to the metal's dimensions, and substrates (especially silicon) are lossier. Capacitors can be lossy, compared to discrete chips, in part because of greater dielectric losses.

Both inductors and capacitors have reactive parasitics as well as resistive ones. Parasitics are almost always significant in high-frequency, lumped-element matching circuits, so they must be included in the circuit design.

7.1.4.3 Microstrip Losses

Microstrip transmission lines are used for circuit-board interconnections as well as for matching-circuit elements. Losses in microstrip arise in the metal's resistivity and in dielectric losses in the substrate. Modern substrate materials used in hybrid circuits have low loss, so metal losses invariably dominate. The same is largely true of microstrips in GaAs and InP ICs; in silicon ICs, however, the dielectric is notoriously lossy. Microstrip lines can also radiate, especially from such discontinuities as large steps in width and from the ends of open-circuit stubs.

A number of phenomena affect the losses in microstrip transmission lines. The first is simply the resistance of the line. A wider line has lower resistance, but also a lower characteristic impedance, so, for a given power, current is greater. In spite of the increased current, however, losses in practical microstrip media generally increase with decreasing line width. Thin substrates and high dielectric constants (ε_r) result in relatively narrow lines for a given characteristic impedance. Conversely, thick substrates and low ε_r allow for wide, low-loss lines; composite materials, having ε_r in the range of 2 to 4, and fused silica, having $\varepsilon_r = 3.8$, are often preferred for low-noise amplifiers. Radiation increases, however, with thick substrates at high frequencies, and generation of higher-order modes in the lines and discontinuities is also possible.

Use of a thick metallization, up to a thickness of three skin depths, also helps to minimize loss. Because currents in microstrip lines are concentrated at the edges and undersides of the strip, edge and substrate roughness

can increase the transmission-line loss. Chemical etching of the substrate can cause significant edge roughness; depositing the metal by sputtering or electroplating, or etching by ion milling, results in smoother edges. Substrate roughness can be avoided through the use of polished ceramic or inherently smooth materials, such as fused silica or sapphire.

The problem of roughness is especially severe in edge-coupled transmission lines, where edge currents are especially high and strips are often narrow. This problem arises frequently in quadrature-coupled amplifiers, where multistrip Lange couplers are used. When realized on 635-μm alumina substrates, the strip widths and spacings of such couplers are on the order of 60 μm. Depending on frequency, midband excess losses of 0.5 dB or more in the couplers alone are often observed.

The current densities in microstrip matching circuits can be surprisingly nonuniform. Certain parts of a matching circuit may have locally high current densities, while the currents in other parts are very low. A modest reduction in loss can be achieved by designing the matching circuit to minimize such hot spots; suspect areas are the inside corners of T junctions and angular bends. These often can be smoothed to improve the current uniformity. A planar electromagnetic simulator can be helpful in finding such problems.

7.1.4.4 Other Transmission Media

Other transmission media, for example, stripline or suspended substrate stripline, have occasionally been used in low-noise amplifiers. These media often have the advantage of lower loss than microstrip, but they usually are less practical. For this reason, these media have been used only occasionally, mainly for such special-purpose applications as space hardware or radio astronomy.

One structure, occasionally used for high-frequency amplifiers, is microstrip in a channel, in which a microstrip line on a thick, low-ε_r substrate is mounted in a U-shaped channel in a metal housing. This has many of the characteristics of microstrip and stripline, while allowing easy access to the strip for tuning and mounting of chip components.

The high input VSWR of a low-noise amplifier can increase the losses in the coaxial line or waveguide at the input of the amplifier. If the line is longer than one-half wavelength, the high-current regions in its standing-wave pattern have disproportionately high loss. Whatever the input VSWR, coaxial lines have relatively high loss, compared to interconnection media such as waveguide, so their use at the amplifier input must be minimized.

7.1.5 Extraneous Noise Sources

Noise can be inadvertently applied to an amplifier from other sources. One of the most common is the bias circuitry.

Frequently, dc bias (especially gate bias in a FET amplifier) is applied through a large-value resistor. This resistor has a number of beneficial properties: it can improve stability, improve input match, and limit the increase in gate current when a strong signal is applied to the amplifier. The resistor's value is selected to have minimal effect on the gain and input impedance.

Depending on the FET and the resistor's value, the resistor's noise may increase the amplifier's noise figure. If the resistor's value is much greater than the input impedance at the point where it is connected, the noise current injected into the circuit is relatively small. This case is illustrated in Figure 7.5. Z_p is the impedance measured at the point where the resistor is connected [the parallel combination of Z_d and Z_s in Figure 7.5(a)]. We assume that $R_{bb} \gg |Z_p|$; if it were not, the increased input loss would have an obvious and disastrous effect on the noise figure. Since R_{bb} then has negligible effect on matching, we can treat the device noise as a noise temperature, modeled by a noise source associated with its source impedance. This source is v_{ns} in the figure. The FET itself is then noiseless.

A simple analysis shows the mean-square noise voltage applied to the input of the device to be

$$\overline{|v_n|^2} = 4KT_p \frac{|Z_p|^2}{R_{bb}} \tag{7.14}$$

where T_p is the physical temperature of the resistor and R_{bb} is its resistance. In deriving (7.14), we observe that, although the open-circuit noise voltage of the resistor increases with R_{bb}, the voltage at the device input decreases as $1/R_{bb}$. To find the increase in noise temperature caused by R_{bb}, we replace the FET gate in Figure 7.5(b) with a short circuit (since the FET, in the equivalent circuit, is noiseless) and calculate the short-circuit output currents. The result is

$$\Delta T_n = T_p \frac{|Z_s|^2}{R_{bb}\,\mathrm{Re}\{Z_s\}} \tag{7.15}$$

showing that the increase in noise temperature is negligible when $R_{bb} \gg |Z_s|^2 / \mathrm{Re}\{Z_s\}$. Z_s is usually well known, as it is an approximation of the device's optimum source impedance.

Another potential source of noise is an active bias circuit. Active circuits can generate fairly high levels of noise, which can be surprisingly broadband. It is especially important to decouple them well from the amplifier's input.

Any type of stray pickup from environmental noise sources can increase the noise temperature of a very low-noise receiver (Section 3.3.4.5). The noise can enter the amplifier through an inadequately shielded housing

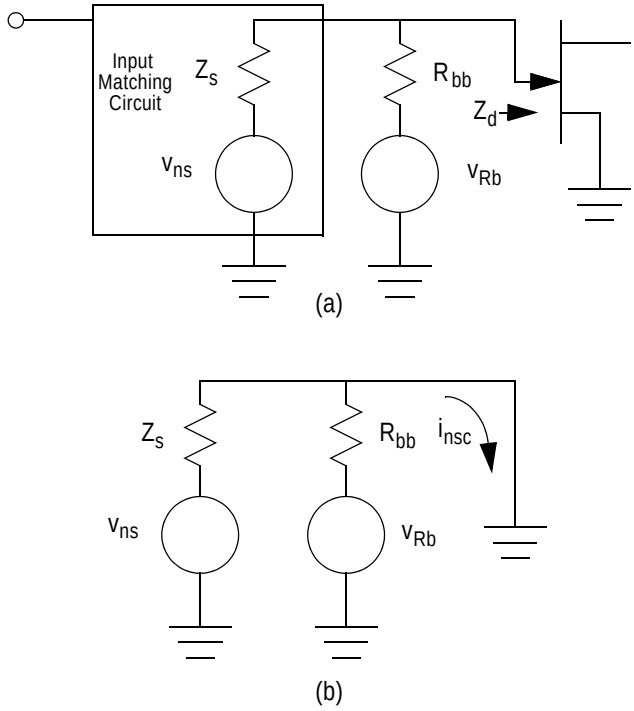

Figure 7.5 (a) Noise equivalent circuit of the input of an amplifier with a resistor used for bias insertion. The noise temperature of the amplifier is modeled by a noise source in series with the transformed source impedance; $\overline{|v_{ns}|^2} = 4KT_n\Delta f\,\mathrm{Re}\{Z_s\}$. (b) Equivalent circuit used to determine the increase in noise temperature caused by R_{bb}.

or via inadequately bypassed dc leads. Such receivers require great care in the design of their housings and dc circuitry.

7.1.6 The Input VSWR Problem

The need for a mismatched input creates a difficulty in the use of a low-noise amplifier in an RF or microwave system, where matched interfaces are often needed. The input mismatch can introduce gain ripple in the system's passband and increase the loss in an interconnecting cable or waveguide, thus increasing the system's noise figure. Three common methods for improving the input VSWR are feedback, an input isolator, and quadrature-coupled amplifiers.

Some of these methods affect both the input and output VSWR. In general, a high output VSWR is less of a problem than a high input VSWR, because the effect of additional losses introduced by isolators or quadrature hybrids, used to ameliorate the situation, are not as severe. We shall see, in Section 7.2.2, that the need for broad bandwidth inevitably results in high output VSWR over part of the band, and thus some method of VSWR improvement is needed at the output as well as the input.

7.1.6.1 Feedback

Reactive feedback does not decrease the noise figure to any practical degree. A classic paper by Haus and Adler [7.2] showed generally that the noise *measure* of a transistor remains constant, even when $F_{\min}$ decreases.[1] Feedback can change $Y_{s,\,\mathrm{opt}}$ to a more desirable value, however, to facilitate the design of the input matching circuit.

In particular, inductive feedback in the source terminal of a FET increases the real part of the input impedance, making it possible to match the device simultaneously for both noise and VSWR. Such matching is, unfortunately, relatively narrowband and can affect stability. The synthesized real component of input impedance is noiseless.

A simple analysis of a FET input circuit with source-lead inductance shows that the input impedance is increased by

1. This piece of conventional wisdom, while generally correct in practical applications, may not be strictly true in theory. Series inductive feedback can sometimes reduce $F_{\min}$ while making the device conditionally stable. The maximum gain is then theoretically unlimited, so the noise measure equals $F_{\min}$. When this occurs, most other aspects of the performance are poor (e.g., R_n is large and $|S_{12}|$ is great), so achieving improved noise figure, in practice, may not be possible.

$$\Delta Z_{\text{in}} = g_m \frac{L}{C_{gs}} + Lj\omega \tag{7.16}$$

where ΔZ_{in} is the increase in impedance and L is the source inductance. Although the increased $\text{Re}\{Z_{\text{in}}\}$ is welcome, it is often accompanied by increased R_n, S_{12}, and S_{22}, all of which are undesirable.

7.1.6.2 Isolators

Isolators represent a brute-force approach to the improvement of input VSWR. Isolators that have coaxial connectors are usually realized in stripline; waveguide isolators use ferrite loaded waveguide junctions. Isolators are large, heavy, costly, and introduce at least a few tenths of one decibel of additional input loss. An isolator is needed on each port that requires VSWR improvement.

Microstrip isolators, which can be mounted inside the amplifier package, are also available. These are much smaller than stripline or waveguide isolators but have greater loss. Because of the difficulty of making connections to them, they usually do not provide as good VSWR as the other types.

7.1.6.3 Quadrature-Coupled Amplifiers

One of the most common configurations for microwave amplifiers of all types is shown in Figure 7.6. In the figure, a pair of ideally identical amplifiers is coupled by quadrature hybrids at both the input and output. The hybrids' isolated ports are terminated. This configuration, first proposed by Englebrecht and Kurokawa [7.3], has a number of useful characteristics. One of the most important is that the input VSWR is ideally 1.0, regardless of the input reflection coefficients of the individual amplifiers, as long as they are identical and the hybrids are ideal. Even with the limitations that reality places upon such components, however, low input VSWR can still be achieved over a broad bandwidth.

It is easy to see why this occurs by considering the input hybrid in Figure 7.6. An ideal quadrature hybrid has the scattering matrix,

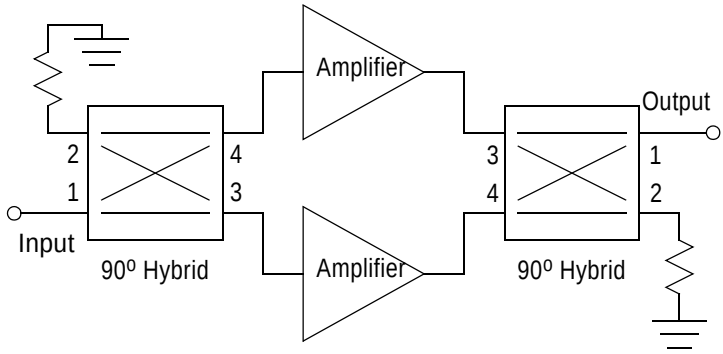

Figure 7.6 Quadrature-coupled amplifiers. The port numbering of the hybrids is for reference in the text.

$$\mathbf{S}_{90} = \frac{1}{\sqrt{2}} \begin{bmatrix} 0 & 0 & -j & 1 \\ 0 & 0 & 1 & -j \\ -j & 1 & 0 & 0 \\ 1 & -j & 0 & 0 \end{bmatrix} \tag{7.17}$$

showing that the paths through the hybrid have 3-dB loss and either 0- or 90-degree phase shift. (The phase shift through real hybrids is much greater; the difference between in phase at the output ports is the important quantity; absolute phase delay is not.) Port 1 is the input and ports 3 and 4 are terminated with the reflection coefficient of the amplifiers, Γ, assumed to be equal. The terminations constrain the *a* and *b* waves at ports 3 and 4 to be

$$a_3 = \Gamma b_3 \tag{7.18}$$

and

$$a_4 = \Gamma b_4 \tag{7.19}$$

Substituting (7.18) and (7.19) into (7.17) gives

$$\begin{bmatrix} b_1 \\ b_2 \end{bmatrix} = \Gamma \begin{bmatrix} 0 & -j \\ -j & 0 \end{bmatrix} \begin{bmatrix} a_1 \\ a_2 \end{bmatrix} \tag{7.20}$$

Port 2 has an ideal termination, so $a_2 = 0$ and therefore $b_1 = 0$. All the power reflected from the individual components is dissipated in the load at port 2, and none emerges from port 1, so the input port is matched. The same applies to the output port, which is also matched. When the terminations on ports 3 and 4 are unequal and the termination on port 2 is ideal, we can derive, similarly,

$$\Gamma_{in} = 0.5(\Gamma_3 - \Gamma_4) \tag{7.21}$$

where $\Gamma_{in} = b_1/a_1$, and Γ_3, Γ_4 are the input reflection coefficients of the two amplifiers terminating ports 3 and 4, respectively. We see that, even when the port terminations are not precisely equal, the input VSWR may still be very low.

The quadrature couplers in microwave amplifiers are realized as coupled-line structures. Because it is impossible to achieve adequate coupling in microstrip between a single pair of lines, four or more strips are used and the conductors are interleaved. These so-called *Lange hybrids* also use a clever arrangement to create a crossover in the center of the coupler, placing the input and output ports in the desired locations. Quadrature-coupled amplifiers are almost always realized in microstrip on alumina substrates, as the high dielectric constant (approximately 9.6 to 10.0, depending upon manufacturing methods) provides small size and adequate coupling. See [7.4] for further information on such couplers.

An ideal coupled-line hybrid's port VSWR, phase balance, and isolation are theoretically perfect and frequency independent. Its amplitude balance is imperfect, however, varying as $\sin^2(\pi\omega / 2\omega_0)$, where ω_0 is its center frequency. This imperfection is not as important as it may seem at first, because, if the loss from the input to one port of the hybrid is c ($c < 1$), the loss from the input to the other port must be $1 - c$. Figure 7.6 shows that a signal passing through one branch of the circuit must experience loss c through one hybrid and loss $1 - c$ in the other. The couplers largely compensate each other, giving the amplifier surprisingly flat gain, even at frequencies where the coupler's balance is poor. Furthermore, for broadband operation, the couplers can be overcoupled at bandcenter to minimize the worst-case imbalance at the band edges.

A great concern, for our purposes, is the noise from the termination connected to the unused port of the input coupler. This noise is applied to the inputs of the amplifiers, so at first appearance, the noise temperature must increase by the temperature of this termination. However, the noise from the resistor is correlated in the amplifiers' outputs, so it is subtracted by the output coupler. Ideally, none of the termination's noise reaches the output.

The termination noise can reach the output only if the hybrids are not perfectly balanced. The increase in output noise temperature arising from amplitude imbalance between the in-phase and quadrature-phase paths through the hybrids is

$$\Delta T_{nL} = G_{ta} T_t (2c - 1)^2 \tag{7.22}$$

where ΔT_{nL} is the increase in output noise temperature, T_t is the termination's physical temperature, G_{ta} is the amplifiers' gain (i.e., the amplifier blocks alone, not including the hybrids), and c is either hybrid's power coupling factor at the frequency of interest, which generally deviates from the ideal bandcenter value of 0.5. In (7.22), we assume the phase balance to be perfect; in fact, phase imbalance in practical hybrids is minor, so amplitude imbalance dominates. The imbalance reduces the gain of the complete amplifier to $4G_{ta}c(1-c)$, so the increase in the input noise temperature, ΔT_n, is

$$\Delta T_n = \frac{T_t (2c - 1)^2}{4c(1 - c)} \tag{7.23}$$

Even this is a relatively minor increase in noise temperature in most cases.

The coupling loss has no effect on the noise figure of the amplifier; if the coupler is ideal, the noise figure of the coupled amplifiers is the same as that of the individual amplifiers. However, excess loss in the coupler, caused by resistive losses in the microstrip, increases the noise figure of the amplifier in the same manner as any input attenuation (Section 7.1.4.3). The excess coupler loss, combined with the loss in relatively narrow microstrips, can be significant. Thus, such amplifiers do not achieve the lowest possible noise figures.

7.1.6.4 Output Loading

It is well known that the output load of a nonunilateral two-port affects the input reflection coefficient. The input reflection coefficient, Γ_{in}, of a terminated two-port is

$$\Gamma_{\text{in}} = S_{11} + \frac{S_{21}S_{12}\Gamma_L}{1 - S_{22}\Gamma_L} \tag{7.24}$$

where Γ_L is the load reflection coefficient. It seems possible, in some cases, to adjust Γ_L so that Γ_{in} is a conjugate match to $\Gamma_{s,\text{opt}}$. Unfortunately, even when this is possible, it invariably results in a poor output match and gain that is not constant over the desired frequency range. In effect, this technique, when possible at all, simply displaces the VSWR problem from the input to the output. Although this might be an improvement in some cases, the method is suggested in the literature more frequently than used in practice.

7.1.7 Thermal Effects and Cooled Amplifiers

Heating and cooling have obvious effects on the thermal noise sources in low-noise devices. They affect nonthermal sources, and the amplifier's noise figure, in a somewhat indirect manner.

As a FET's temperature increases, its transconductance decreases, partly from increases in parasitic resistance (especially the source-lead resistance) and from a decrease in the electrons' saturation velocity. C_{gs} changes little, so ω_t decreases. G_{nd} increases as well, although part of the increase may come from increased drain current, which is necessary for maintaining adequate transconductance. From (7.11), F must increase with temperature. R_i in (7.11) is a thermal noise resistance, so it must be scaled in proportion to absolute temperature as well.

FET amplifiers (but not bipolar amplifiers) can be cooled to achieve great reductions in noise temperature. For such applications as radio astronomy, which require extremely high sensitivity, FETs are often cooled to cryogenic temperatures. For example, Pospieszalski [7.5] shows a decrease in minimum noise temperature of a factor of approximately 6 for an 8.5-GHz HEMT cooled from 297K to 12.5K. The author has observed noise-temperature reductions of a factor of approximately 3 in cooling a MESFET amplifier from room temperature to 77K.

Maintaining low noise figures of both cooled and room-temperature amplifiers requires care in thermal design and design of the bias networks.

The FET chip or package must have adequate heat sinking, even though the power dissipation at low-noise bias is rarely very great. To compensate for gain changes, bias circuits often increase dc drain current as temperature increases. This kind of compensation, if not performed carefully, can increase the noise figure significantly.

Both the noise and S parameters of a FET change markedly with decreasing temperature. Ideally, the amplifier should be designed according to the low-temperature S and noise parameters, and any manual tuning should be performed at the low temperature. Because of the practical difficulty of measuring S and noise parameters at very low temperatures, amplifiers intended for low-temperature operation are often designed according to room-temperature design data. The improvement on cooling such amplifiers is probably not as great as theoretically possible, but still significant.

7.2 AMPLIFIER OPTIMIZATION

In this section we address the problem of optimizing the noise performance of amplifiers. We focus entirely on aspects of low-noise design; we do not discuss the basics of amplifier design, as that subject is well covered in other texts.

7.2.1 Narrowband Amplifiers

7.2.1.1 Fundamental Considerations

The design of narrowband amplifiers—amplifiers having bandwidths of perhaps 10% or less—is straightforward. The input matching circuit is designed to present the optimum source admittance, $Y_{S,\,\mathrm{opt}}$, to the transistor; the output impedance, with the optimum noise admittance loading the input, is then calculated. Finally, the output circuit is designed to achieve a conjugate match. Designing these circuits at the center frequency usually provides adequate performance over the required bandwidth.

A perennial problem in the design of narrowband amplifiers is high gain outside of the desired band, especially at low frequencies. This characteristic is generally undesirable, as it leads to instability and allows interference from strong, out-of-band signals. Proper design of the matching and bias circuits can minimize this problem; for example, small series capacitors and shunt short-circuit stubs in the matching circuit, and resistive loading in the bias circuit, can reduce low-frequency gain.

7.2.1.2 Example

We now design a 9.5- to 10.5-GHz low-noise amplifier using a conventional high-frequency MESFET. The goal is to achieve a good output match and nearly optimum noise figure over the band. These requirements define the matching circuits, so it is impossible to specify the gain as well. The gain will be whatever results from these matching conditions; we expect it to be approximately 10 dB. The circuit is realized as a microwave hybrid on an alumina substrate, $\varepsilon_r = 9.8$.

The amplifier is designed in the following manner:

1. The first step is to check the stability of the device. The stability factor (K factor) is less than 1.0 at frequencies below 8 GHz, creating a potential for oscillation. We design the bias decoupling circuits to include some resistive loading, which should reduce the out-of-band gain enough to stabilize the amplifier. The bias circuits are designed to decouple those resistors at ~10 GHz, to prevent noise of the bias supplies and loading resistors from increasing the amplifier's noise figure. We find that the resistors improve the stability factor, making $K > 1$ at all frequencies. We also check the S parameters and minimum noise figure to make sure that they have not been changed by the bias circuit or loading resistors.
2. Next, we design the input matching circuit. The goal is to synthesize the source reflection coefficient for optimum noise match. A simple circuit consisting of series lines and open-circuit stubs suffices.
3. With the input matching network in place, we calculate the output reflection coefficient over the band of interest.
4. Finally, we design the output matching network. To minimize low-frequency gain, it includes a shorted stub.

This initial design should be close to optimum, but still may benefit from numerical optimization. An initial result that is far from optimum indicates that an error has been made in the above process; it should be fixed before any further numerical optimization is performed. It is always a bad practice to use an optimizer to fix errors.

The amplifier circuit is shown in Figure 7.7. Figure 7.8(a) shows its gain and output return loss, and Figure 7.8(b) shows its noise figure, the minimum noise figure of the device, and the input return loss. The noise

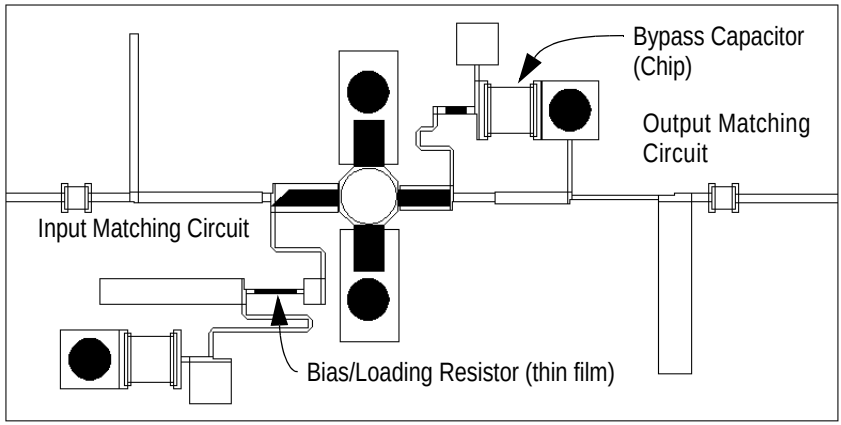

Figure 7.7 Layout drawing of the narrowband amplifier. The input and output use simple stub matching circuits, designed at the center frequency (10 GHz). Although the design bandwidth is 1.0 GHz, good performance is achieved over a 2.0 GHz bandwidth.

figure is approximately 0.5 dB worse than the device's minimum; the increase is largely caused by circuit loss.

The input VSWR is approximately 2.0 worst case, adequate for many applications. It is not difficult to see why the VSWR is unexpectedly good: we are using a mediocre device. As $\omega \rightarrow \omega_t$, the rightmost term in (7.11) becomes dominant, so it is more important to minimize it, by conjugate matching the input, than to minimize the R_i / R_s term.

7.2.2 Broadband Amplifiers

7.2.2.1 The Broadband Amplifier Problem

The need for broad bandwidth creates special problems in the design of low-noise amplifiers. The fundamental problem is the theoretical impossibility of creating a perfect input matching circuit (i.e., one that synthesizes $Y_{s,\,\mathrm{opt}}$ exactly) over a broad bandwidth. We must, instead, tolerate some degree of mismatch, somewhere within the amplifier's passband. In the input circuit, the obvious place to tolerate this mismatch is at the low end of the band, where $F_{\min}$ is lower and there is more room for error.

For the same reasons, we cannot match the output arbitrarily well over a wide bandwidth. In fact, a perfect broadband output match usually is undesirable, as it results in a sloped gain, lower at the high-frequency end of

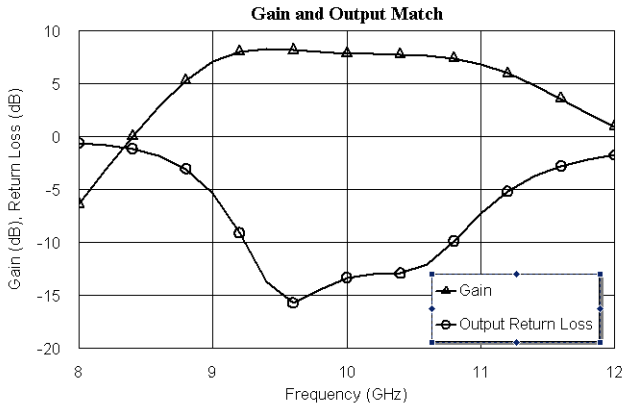

(a)

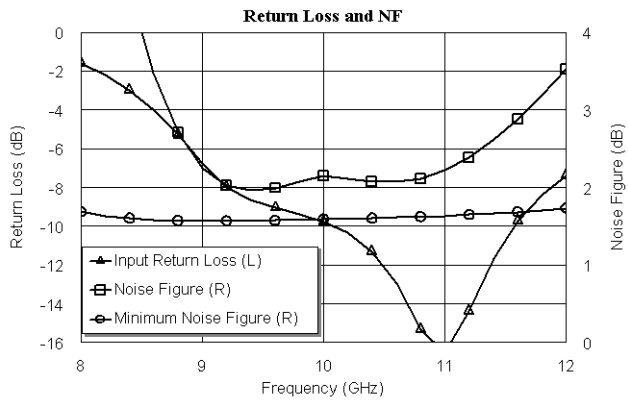

(b)

Figure 7.8 Performance of the narrow-band amplifier: (a) gain and output return loss; (b) input return loss and noise figure compared to the device's $F_{\min}$.

the band than at the low-frequency end. Instead, we purposely mismatch the low end of the band to achieve flat gain over the desired passband.

The fundamental problem becomes one of designing the matching circuits to achieve these goals, along with the usual requirements of stability and low out-of-band gain. This can be a complicated task. One approach is to determine a set of source and load impedance loci that provide the desired performance and can be modeled simply. If such a set can be found, we can then generate the matching circuits in a straightforward manner. Fortunately a technique called *negative-image modeling* can accomplish this. We describe the method in the following section.

7.2.2.2 Negative-Image Modeling

The design of the input circuits for broadband amplifiers requires competing trade-offs between gain and noise. The fundamental problem is to determine an appropriate, realizable set of source and load reflection coefficients, over the band of interest, that optimizes all requirements of the amplifier. The method described here, first proposed by Medley and Allen in 1979 [7.6], is both elegant and practical.

The method is as follows:

1. We first create a circuit having the special negative-image source and load networks as shown in Figure 7.9(a). $-C_S$ and $-C_L$ are negative capacitances. These networks can have any structure, but, to facilitate the synthesis of the real networks, they should be as simple as possible. The source network should approximate the locus of $\Gamma_{S,\,\mathrm{opt}}$ and the output network should mirror the structure of the device's drain equivalent circuit.
2. We then optimize the circuit by means of a linear circuit-analysis program, using whatever trade-offs are appropriate. Because of the negative capacitances, the optimization is surprisingly easy.
3. When satisfactory performance has been achieved, we synthesize input- and output-matching networks using loads that are the positive versions of the negative-image networks [Figure 7.9(b)]. This is best accomplished by a circuit-synthesis program, but any other favored method can be used.
4. We replace the negative-image circuits with the matching circuits and do any necessary final optimization.

If the matching circuits synthesized in Figure 7.9(b) provided a conjugate match to their respective positive-load networks, their output impedances would be exactly equal to those of the negative-image networks. Even though a perfect conjugate match is not possible, the networks still provide a good approximation of the optimum source and load reflection coefficients, Γ_s and Γ_L, of those networks.

7.2.2.3 Example

The process of negative-image modeling is best described by a design example. We wish to design an 8- to 12-GHz low-noise amplifier. We begin by creating the negative-image model shown in Figure 7.10. This model may require a little experimentation; a series RC at the input and a parallel RC at the output usually work well, but in this case, we use a parallel RLC at the output. We optimize the circuit using these negative-image networks; the optimization emphasizes whatever aspects of the performance are im-

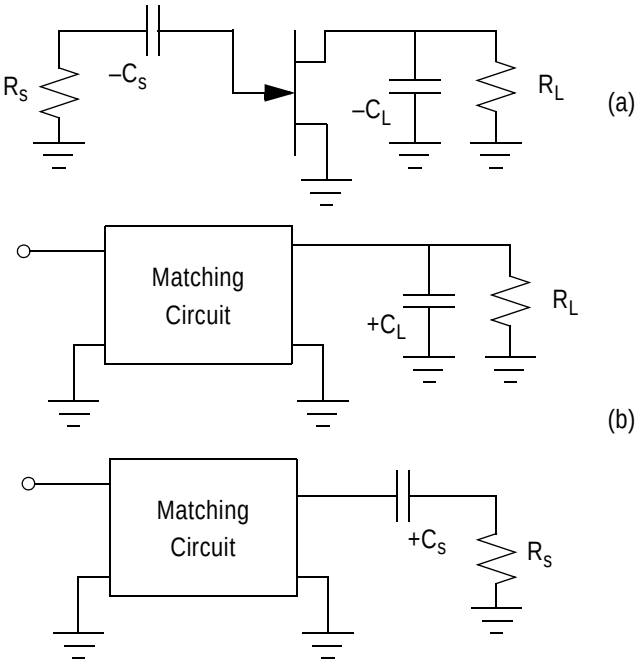

Figure 7.9 Negative-image matching: (a) a FET with negative-image networks; (b) synthesis of equivalent real matching circuits.

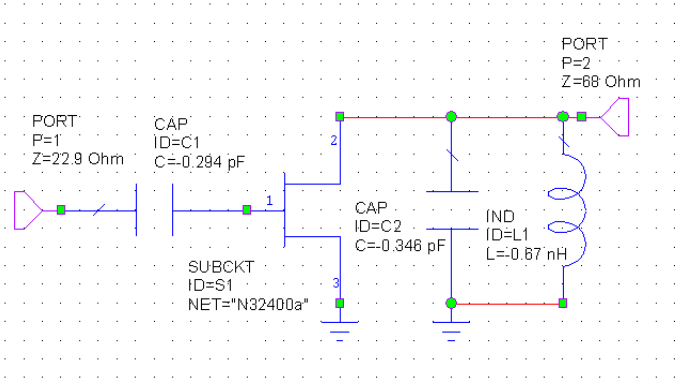

Figure 7.10 The optimized negative-image model of the amplifier.

portant for the amplifier's application. The next step is to synthesize the matching circuits, which is accomplished with the help of circuit-synthesis software. Finally, we add the synthesized circuits to the FET and do any final optimization deemed necessary.

The result, compared to the performance of the negative-image model, is shown in Figure 7.11. The midband gain of the finished amplifier is quite close to the negative-image model, but it rolls off somewhat at the high end of the band. The noise figure is largely as expected; it follows the negative image model over most of the band, diverging most strongly at the lower edge. Numerical optimization of the finished amplifier could further improve the performance.

The critical part of the design is the optimization of the circuit in Figure 7.10. The characteristics of this circuit, including stability, noise figure, gain, and all other parameters of interest are, within the limitations of matching-network synthesis, those of the resulting amplifier. The trade-offs at this stage of the design can be whatever the designer deems appropriate; usually, the negative-image model is designed with the help of numerical optimization. The goals and weights of the optimized parameters determine the performance of the finished amplifier.

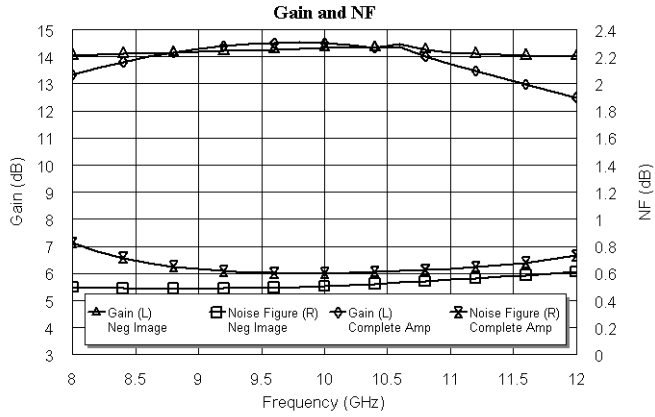

Figure 7.11 Comparison of the gain and noise figure of the finished amplifier to that of the negative-image model.

References

[7.1] E. W. Strid, "Measurement of Losses in Noise Matching Networks," *IEEE Trans. Microwave Theory Tech.*, Vol. MTT-29, p. 247, 1981.

[7.2] H. A. Haus and R. B. Adler, "Optimum Noise Performance of Linear Amplifiers," *Proc. IRE*, Vol. 46, p. 1517, 1958.

[7.3] R. S. Englebrecht and K. Kurokawa, "A Wide-Band, Low-Noise L-Band Balanced Transistor Amplifier," *Proc. IEEE*, Vol. 53, p. 237, 1965.

[7.4] R. Mongia, I. Bahl, and P. Bhartia, *RF and Microwave Coupled-Line Circuits*, Norwood, MA: Artech House, 1999.

[7.5] M. W. Pospieszalski, "Modeling of Noise Parameters of MESFETs and MODFETs and Their Frequency and Temperature Dependence," *IEEE Trans. Microwave Theory Tech.*, Vol. MTT-37, p. 1340, 1989.

[7.6] M. Medley and J. L. Allen, "Broad-Band GaAs FET Amplifier Design Using Negative-Image Device Models," *IEEE Trans. Microwave Theory Tech.*, Vol. 27, p. 784, 1979.